

PAPER

Investigation of normal and superconducting states in noncentrosymmetric $\text{Re}_{24}\text{Ti}_5$

To cite this article: C S Lue *et al* 2013 *Supercond. Sci. Technol.* **26** 055011

View the [article online](#) for updates and enhancements.

You may also like

- [Study on influencing factors of microbial induced carbonate precipitation in a cross fracture network](#)
L Guo, M Liao, Y Peng et al.
- [Properties and Structure of Electroless Deposited Rhenium-Rich Re-Co Thin Films](#)
Alexandra Inberg
- [Rhenium Electrodeposition to Enable Functionally Graded Films](#)
Michael McBride, Courtney L Clark, Daniel E Hooks et al.

Investigation of normal and superconducting states in noncentrosymmetric $\text{Re}_{24}\text{Ti}_5$

C S Lue¹, H F Liu¹, C N Kuo¹, P S Shih², J-Y Lin², Y K Kuo³,
M W Chu⁴, T-L Hung⁵ and Y Y Chen⁵

¹ Department of Physics, National Cheng Kung University, Tainan 70101, Taiwan

² Institute of Physics, National Chiao Tung University, Hsinchu 30010, Taiwan

³ Department of Physics, National Dong Hwa University, Hualien 97401, Taiwan

⁴ Center for Condensed Matter Sciences, National Taiwan University, Taipei 10601, Taiwan

⁵ Institute of Physics, Academia Sinica, Taipei 11529, Taiwan

E-mail: ago@cc.nctu.edu.tw (J-Y Lin) and ykuo@mail.ndhu.edu.tw

Received 19 December 2012, in final form 27 February 2013

Published 4 April 2013

Online at stacks.iop.org/SUST/26/055011

Abstract

We report a detailed characterization of the noncentrosymmetric superconductor $\text{Re}_{24}\text{Ti}_5$ using powder x-ray diffraction (XRD), magnetic susceptibility, electrical resistivity, thermal conductivity, Seebeck coefficient, and specific heat measurements. Rietveld refinement of powder XRD data confirms that $\text{Re}_{24}\text{Ti}_5$ crystallizes in the α -Mn structure. All measured quantities demonstrate a bulk superconducting transition at $T_c = 5.8$ K. Our low-temperature specific heat data measured down to 0.5 K yield a Sommerfeld coefficient $\gamma = 111.8 \text{ mJ mol}^{-1} \text{ K}^{-2}$, which implies a high density of states at the Fermi level. Moreover, the electronic specific heat in the superconducting state was found to obey a typical s-wave expression, revealing a single gap $\Delta/k_B = 10.6$ K. This value gives a ratio of $2\Delta/k_B T_c = 3.68$, higher than the value of 3.5 predicted from BCS theory. On this basis, we conclude that the noncentrosymmetric $\text{Re}_{24}\text{Ti}_5$ compound can be characterized as a moderately coupled BCS-type superconductor. Furthermore, the obtained parameters from the present study of $\text{Re}_{24}\text{Ti}_5$ were compared to those of the isostructural compound $\text{Re}_{23.8}\text{Nb}_{5.2}$, indicating the similarity between both systems.

(Some figures may appear in colour only in the online journal)

1. Introduction

The physics of noncentrosymmetric systems continues to attract attention because of the association with the Rashba-type antisymmetric spin-orbit coupling (ASOC) that may be enhanced in the superconducting (SC) materials where the atomic sites lack spatial inversion symmetry [1–4]. The enhancement of ASOC would lead to the lifting of spin degeneracy and thus the splitting of the energy bands. As a consequence, the superconducting order parameter does not have definite parity but may appear as a mixture of the spin singlet and triplet states [1–4]. Superconductors such as CePt_3Si , CeIrSi_3 , Re_3W , $\text{Re}_{24}\text{Nb}_5$,

$\text{Mo}_3\text{Al}_2\text{C}$, BiPd , ...etc, [5–14] have been reported to possess noncentrosymmetric characteristics. Among these rare-earth and transition metal based noncentrosymmetric superconductors, the d-electron systems are more suitable for exploring the issue of inversion symmetry breaking because the strong electron correlations in f-electron containing materials usually complicate the superconducting properties.

$\text{Re}_{24}\text{Ti}_5$, which crystallizes in a cubic α -Mn structure with the space group $I\bar{4}3m$ (No. 217) [15], belongs to the group of noncentrosymmetric systems. Together with its superconductivity discovered in the 1960s [16–19], this material could be classified as a noncentrosymmetric superconductor. While $\text{Re}_{24}\text{Ti}_5$ has been reported to be a

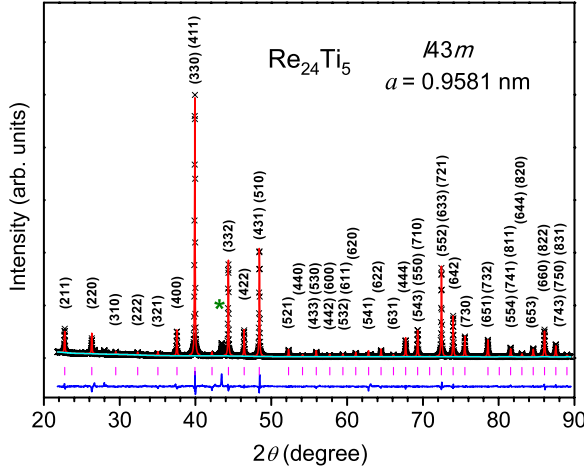


Figure 1. Rietveld refinement of the powder x-ray diffraction data from $\text{Re}_{24}\text{Ti}_5$ shows the main $I\bar{4}3m$ phase with a minor impurity peak arising from TiO_2 marked by the asterisk. The experimental data are presented by the cross symbols. The difference between the experimental and the refined pattern is shown as the lower continuous line.

superconductor, the nature of its superconductivity and other normal state properties remain unexplored. Within the $I\bar{4}3m$ phase, there are two nonequivalent crystallographic titanium sites and two rhenium sites in $\text{Re}_{24}\text{Ti}_5$. Among them, only the Ti(1) site (2a in Wyckoff notation) displays an inversion center. It is of great importance that $\text{Re}_{24}\text{Ti}_5$ contains more than 80% heavy Re atoms which may promote a strong ASOC effect in its SC state. In this respect, $\text{Re}_{24}\text{Ti}_5$ would provide an opportunity to search for the existence of a mixture of spin singlet and spin triplet states in the SC phase of the noncentrosymmetric compounds.

In this paper, we report on the synthesis and characterization of $\text{Re}_{24}\text{Ti}_5$, which exhibits a distinct bulk SC transition at $T_c \simeq 5.8$ K. Measurements of the magnetic, transport, and thermal properties have been performed. From these experimental results, we determined various SC parameters and normal state physical quantities. The observations in the SC phase can be described well by means of the moderately coupled BCS-type superconductivity for $\text{Re}_{24}\text{Ti}_5$. In addition, the obtained parameters were compared to those of the isostructural superconductor $\text{Re}_{23.8}\text{Nb}_{5.2}$ (termed as $\text{Re}_{0.82}\text{Nb}_{0.18}$ in [9]). Strong similarities between both compounds were found, pointing to the similar SC and normal state characteristics among the $\text{Re}_{24}\text{Ti}_5$ -type noncentrosymmetric superconductors.

2. Experimental results and discussion

A nominally stoichiometric $\text{Re}_{24}\text{Ti}_5$ sample was prepared from 99.997% Re and 99.95% Ti by mixing appropriate amounts of elemental metals. They were placed in a water-cooled copper crucible and then melted several times in an Ar arc-melting furnace. The resulting ingot was annealed in a vacuum-sealed quartz tube at 800 °C for five days, followed by furnace cooling. A room-temperature x-ray diffraction analysis taken with Cu K α radiation on the powdered sample

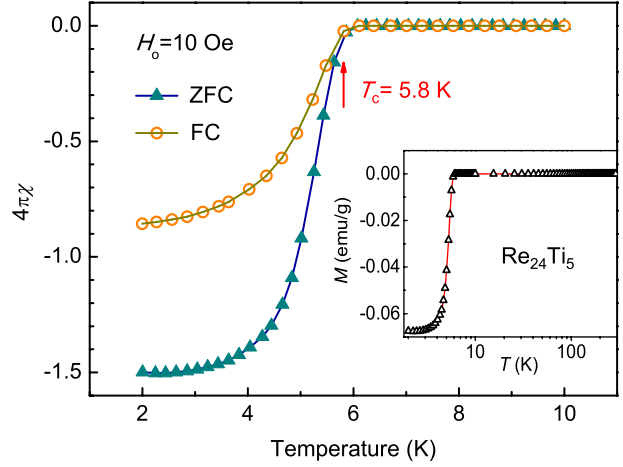


Figure 2. Temperature dependence of magnetic susceptibility under zero-field-cooled (ZFC) and field-cooled (FC) processes for $\text{Re}_{24}\text{Ti}_5$ measured at $H_o = 10$ Oe. The inset displays a plot of M versus T in both superconducting and normal states.

is shown in figure 1. It is seen that the diffraction spectrum in this material is identical to the expected structure, with a minor impurity peak arising from TiO_2 which has little effect on the superconducting nature of $\text{Re}_{24}\text{Ti}_5$. In a more detailed analysis of the x-ray data, the $I\bar{4}3m$ phase was refined with the Rietveld method. The extracted lattice constant $a = 9.581 \text{ \AA}$ is smaller than that of $\text{Re}_{24}\text{Nb}_5$ ($a = 9.6076 \text{ \AA}$) [10], in agreement with the fact that Nb has a larger atomic size than Ti.

DC magnetization M measurements were carried out using a SQUID magnetometer with a small field $H_o = 10$ Oe under zero-field-cooled (ZFC) and field-cooled (FC) processes. The temperature-dependent magnetic susceptibility for $\text{Re}_{24}\text{Ti}_5$ is shown in figure 2. The observed diamagnetic behavior below the transition temperature $T_c \simeq 5.8$ K confirms the occurrence of superconductivity in this material. Here T_c was defined as the onset of the diamagnetic response in the magnetization data, as indicated by the arrow in figure 2. Neglecting the details of the demagnetization effect, the value of $4\pi\chi$ (ZFC) at 2 K exceeding -1 indicates that the shielding volume fraction is almost 100%. As shown in the inset of figure 2, the temperature-independent M in the normal state exhibits a typical Pauli-type paramagnetic feature, being consistent with the ordinary metallic characteristic for $\text{Re}_{24}\text{Ti}_5$.

Data of the electrical resistivity ρ were obtained using a standard four-point probe method. The observed temperature dependence of the electrical resistivity for $\text{Re}_{24}\text{Ti}_5$ is displayed in figure 3. Upon decreasing temperature, ρ exhibits metallic behavior, with zero resistivity appearing below T_c . The normal state resistivity between 6.5 and 14 K can be described well by a power law

$$\rho(T) = \rho_o + AT^2, \quad (1)$$

where ρ_o is the residual resistivity and A is the temperature coefficient of the electric resistivity. In the inset of figure 3, we show the plot of $\rho(T)$ versus T^2 , with the linear relation

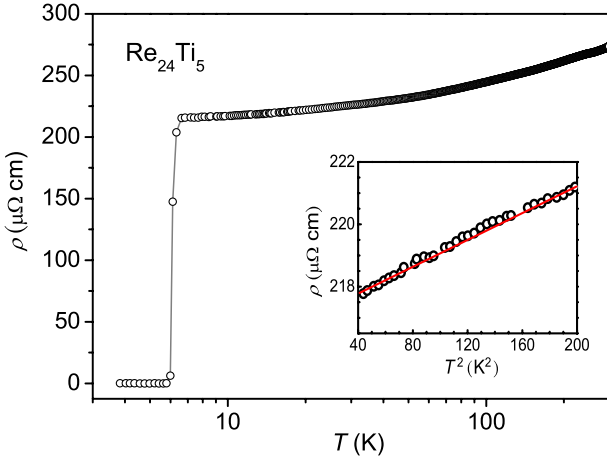


Figure 3. Electrical resistivity as a function of temperature for $\text{Re}_{24}\text{Ti}_5$. Inset: a plot of ρ versus T^2 , showing a linear relation between 6.5 and 14 K.

yielding $\rho_o = 214.8 \mu\Omega \text{ cm}$ and $A = 0.022 \mu\Omega \text{ cm K}^{-2}$. It is instructive to mention that the electron–electron scattering rate at low temperatures should grow as T^2 in the Fermi liquid picture while the residual resistivity ρ_o may arise from electron scattering due to domain boundaries and/or defects. The value of ρ_o provides an estimate of the residual resistivity ratio (RRR, $\rho(300 \text{ K})/\rho_o$) of about 1.3 for $\text{Re}_{24}\text{Ti}_5$. This result is similar to those of the α -Mn-type compounds Re_3W (RRR ~ 1.1) and $\text{Re}_{23.8}\text{Nb}_{5.2}$ (RRR ~ 1.3) [8, 9], suggesting that the small RRR is a common feature for the Re-based superconductors with the noncentrosymmetric α -Mn crystal structure.

Thermal conductivity (κ) and Seebeck coefficient (S) experiments were simultaneously performed in a closed cycle refrigerator using a heat pulse technique. Further details of the experimental techniques for these measurements can be found elsewhere [20]. The temperature dependence of the observed thermal conductivity for $\text{Re}_{24}\text{Ti}_5$ is shown in figure 4. No anomalous feature at or below T_c can be detected to the lowest measured temperature, indicating that the heat transport is insensitive to the electron condensation in $\text{Re}_{24}\text{Ti}_5$. However, $\kappa(T)$ shows a clear shoulder near 50 K, commonly seen in solids at low temperatures due to phonon processes. In principle, the total thermal conductivity for an ordinary metal is the sum of electronic and lattice terms. The electronic thermal conductivity (κ_e) can be evaluated using the Wiedemann–Franz law $\kappa_e \rho / T = L_o$, where ρ is the experimental dc electric resistivity and $L_o = 2.45 \times 10^{-8} \text{ W } \Omega \text{ K}^{-2}$ is the theoretical Lorentz number. The extracted T -dependent κ_e for $\text{Re}_{24}\text{Ti}_5$ is displayed as a solid curve in figure 4. The lattice thermal conductivity (κ_L), obtained by subtracting κ_e from the observed κ , is plotted as a dotted curve in figure 4. From this simple estimation, the electronic thermal conductivity is found to be about one third of the total thermal conductivity, reasonable for the good metallic nature of $\text{Re}_{24}\text{Ti}_5$.

Figure 5 illustrates the temperature dependence of the Seebeck coefficient for $\text{Re}_{24}\text{Ti}_5$. The sign of S is positive, signifying that the hole-type carriers dominate the

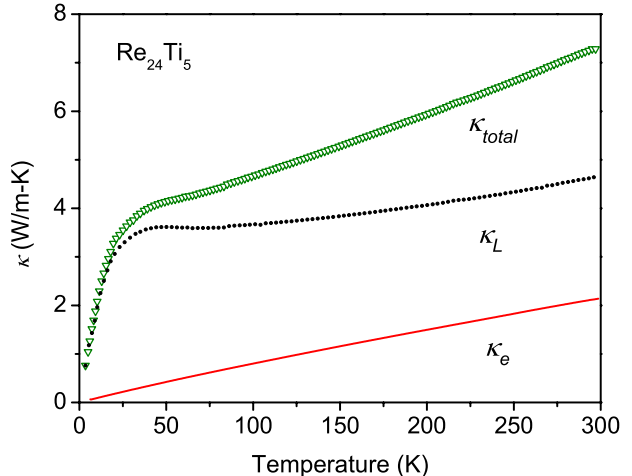


Figure 4. Temperature variation of the thermal conductivity for $\text{Re}_{24}\text{Ti}_5$. Solid and dotted curves represent the decomposed electronic (κ_e) and lattice (κ_L) thermal conductivity, respectively.

thermoelectric transport for $\text{Re}_{24}\text{Ti}_5$. The superconducting transition of $\text{Re}_{24}\text{Ti}_5$ manifests itself by the abrupt drop in S , as indicated in the inset of figure 5. The Seebeck coefficient develops a broad minimum at around 70 K which is ascribed to the phonon-drag effect. The phonon-drag peak is commonly observed in metals and is generally active at low temperatures. It is known that the Seebeck coefficient measurement is a sensitive probe of energy relative to the Fermi surface and the results would reveal information about the Fermi level band structure. Between 150 and 300 K, the observed S varies rather linearly with T , indicating that the diffusion thermopower S_d plays an important role within this temperature range. Such an argument was based on the classical formula $|S_d| = \pi^2 k_B^2 T / 2eE_F$, assuming a one-band model with an energy-independent relaxation time [21]. From the slope of $0.019 \mu\text{V K}^{-2}$, we can extract the magnitude of Fermi energy $E_F = 1.93 \text{ eV}$ (corresponding to the Fermi temperature $T_F = 22\,400 \text{ K}$). Note that this value represents a measure from the bottom of the conduction band to the Fermi level. Also the linear temperature dependence of S_d was thus evaluated, shown as a solid straight line in figure 5. In addition to S_d , the remaining part (the dotted curve in figure 5) arising from the phonon-drag effect, termed as S_g , can be obtained by subtracting S_d from the observed S .

The low-temperature specific heat C measurements were performed using a ${}^3\text{He}$ heat-pulsed thermal relaxation calorimeter in the temperature range from 0.5 to 10 K with the application of a magnetic field up to 8 T. The zero-field and 5 T specific heat data of $\text{Re}_{24}\text{Ti}_5$ are shown in figure 6. Each specific heat jump ΔC associated with the superconducting transition is obvious. The upper critical field H_{c2} of $\text{Re}_{24}\text{Ti}_5$ was also obtained from the magnetic-field-dependent specific heat measurement and the variation of $\mu_0 H_{c2}$ with T/T_c is plotted in figure 7. To estimate the magnitude of $\mu_0 H_{c2}(0)$, we exploited the Werthamer–Helfand–Hohenberg (WHH) theory to fit the data [22]. We thus extracted the value of $\mu_0 H_{c2}(0) = 10.75 \text{ T}$ for the present case of $\text{Re}_{24}\text{Ti}_5$. Similar fittings

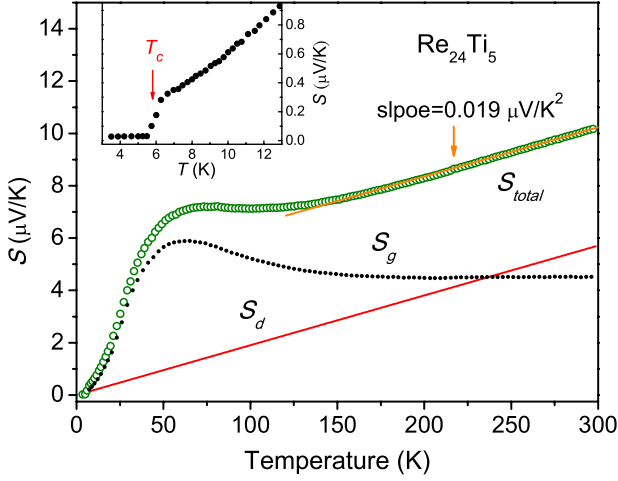


Figure 5. Temperature dependence of the Seebeck coefficient for $\text{Re}_{24}\text{Ti}_5$. A solid line through the observed S data points indicates a linear relation with a slope of $0.019 \mu\text{V K}^{-2}$. Solid and dotted curves represent the decomposed diffusive (S_d) and phonon-drag (S_g) Seebeck coefficient, respectively. The inset shows the Seebeck coefficient data in the vicinity of T_c .

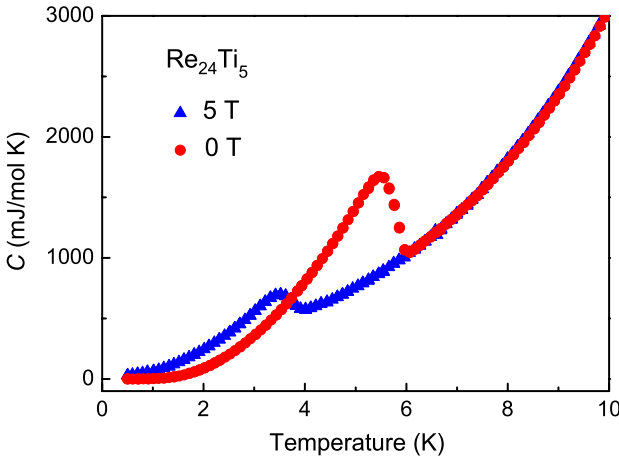


Figure 6. Temperature dependence of the specific heat data measured at $H = 0$ and 5 T for $\text{Re}_{24}\text{Ti}_5$.

have been employed to determine the upper critical field of intermetallic superconductors [9, 23, 24].

The specific heat data above T_c provide an extrapolation of the normal state behavior to $T \rightarrow 0$ and allow the determination of the Sommerfeld constant (γ) and Debye constant (β) from $C(T) = \gamma T + \beta T^3 + \delta T^5$. We thus displayed the plot of C/T versus T^2 at $H = 0$ and 5 T in figure 8, with a solid curve representing the best fit to the experimental data. Such a fit yields $\gamma = 111.8 \text{ mJ mol}^{-1} \text{ K}^{-2}$, $\beta = 1.47 \text{ mJ mol}^{-1} \text{ K}^{-4}$, and $\delta = 0.0049 \text{ mJ mol}^{-1} \text{ K}^{-6}$ for $\text{Re}_{24}\text{Ti}_5$. It should be noted that the magnitude of γ determined from our specific heat measurement is rather high, suggesting the possible high electronic density of states near the Fermi level for this material. Furthermore, the Debye temperature θ_D of 428 K can be evaluated from β using the relation $\theta_D = (12\pi^4 RZ/5\beta)^{1/3}$, where $R =$

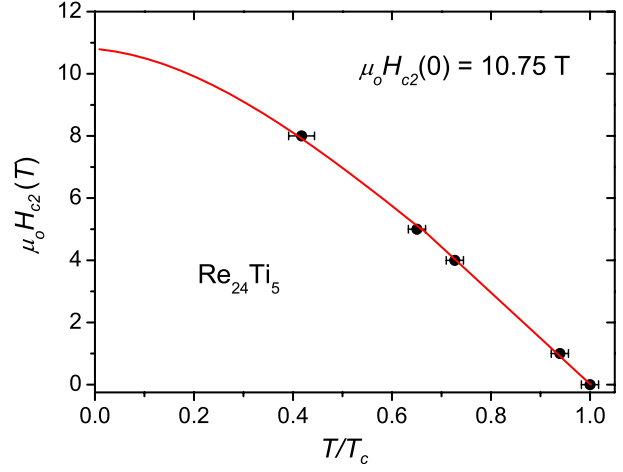


Figure 7. Temperature variation of the upper critical field $\mu_o H_{c2}$ with respect to T/T_c for $\text{Re}_{24}\text{Ti}_5$. The data were determined from the 50% jump of the specific heat. The solid curve is a fitting result according to the Werthamer–Helfand–Hohenberg (WHH) theory.

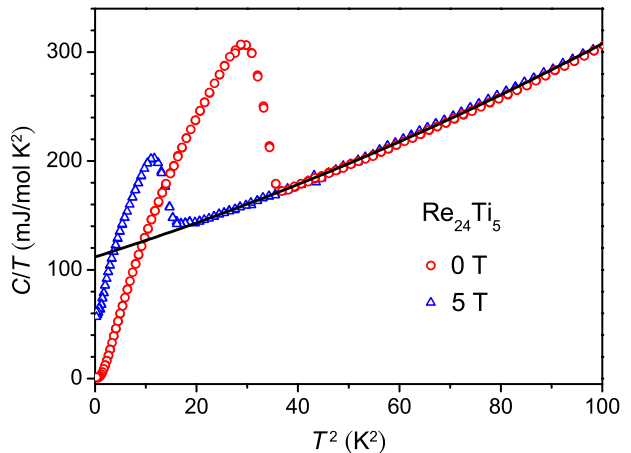


Figure 8. A plot of C/T versus T^2 at $H = 0$ and 5 T for $\text{Re}_{24}\text{Ti}_5$. A linear fit to the experimental data above T_c is a fitting result according to $C(T)/T = \gamma + \beta T^2 + \delta T^4$.

$8.314 \text{ J mol}^{-1} \text{ K}^{-1}$ is the molar gas constant and $Z = 58$ is the number of atoms per unit cell [25].

With these parameters, one can estimate the electron–phonon constant λ_{ep} by means of the McMillan equation [26]

$$\lambda_{ep} = \frac{1.04 + \mu^* \ln \left(\frac{\theta_D}{1.45 T_c} \right)}{(1 - 0.62\mu^*) \ln \left(\frac{\theta_D}{1.45 T_c} \right) - 1.04}. \quad (2)$$

Here μ^* is the Coulomb pseudopotential of about 0.13 used in $\text{Re}_{23.8}\text{Nb}_{5.2}$ and other intermetallic superconductors [9, 27, 28]. Taking $\theta_D = 428$ K and $T_c = 5.8$ K, we obtained $\lambda_{ep} = 0.6$ for $\text{Re}_{24}\text{Ti}_5$. This value is also comparable to those in other fully gapped noncentrosymmetric superconductors, such as 0.66 for $\text{Mg}_{10}\text{Ir}_{19}\text{B}_{16}$ and 0.5 for LaRhSi_3 [29, 30], suggesting that $\text{Re}_{24}\text{Ti}_5$ is a moderately coupled superconductor.

As mentioned, the large γ value in $\text{Re}_{24}\text{Ti}_5$ indicates a high electronic density of states around the Fermi level. The Fermi level density of states $N(E_F)$ can be estimated using the

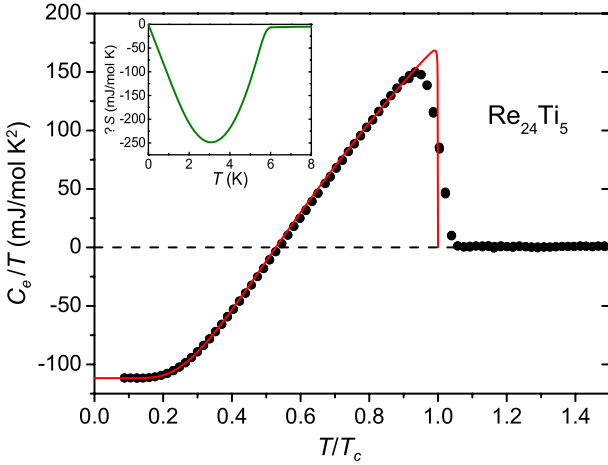


Figure 9. Temperature variation of $C_e(T)/T$ at $H = 0$ with respect to T/T_c for $\text{Re}_{24}\text{Ti}_5$. The solid curve is a theoretical calculation based on the s-wave BCS model. The inset shows the entropy conservation required for a second-order phase transition and justifies the determination of $C(T)$ in figure 8.

values of γ and λ_{ep} according to the relation [25]

$$\gamma = \frac{2\pi^2 k_B^2}{3} N(E_F)[1 + \lambda_{\text{ep}}]. \quad (3)$$

We found $N(E_F) = 14.85$ states eV^{-1} f.u. $^{-1}$ for $\text{Re}_{24}\text{Ti}_5$, larger than the value of 6.56 states eV^{-1} f.u. $^{-1}$ obtained from the same analysis using the data of $\text{Re}_{23.8}\text{Nb}_{5.2}$ [9]. These results were tabulated in table 1. Note that we neglected the contribution from the electronic correlation in equation (3) since this effect is weak in both materials. The argument for the weak electronic correlation is mainly based on the small Kadovski-Woods ratio A/γ^2 . Karki and coworkers have reported a small value of $A/\gamma^2 = 0.24a_0$, where $a_0 = 10^{-5} \mu\Omega \text{ cm mol}^2 \text{ K}^2 \text{ mJ}^{-2}$ for $\text{Re}_{23.8}\text{Nb}_{5.2}$ [9]. Taking $A = 0.022 \mu\Omega \text{ cm K}^{-2}$ and $\gamma = 111.8 \text{ mJ mol}^{-1} \text{ K}^{-2}$, we found $A/\gamma^2 = 0.17a_0$ for $\text{Re}_{24}\text{Ti}_5$, lower than those in typical electronic correlated systems which usually have a magnitude of a_0 for A/γ^2 .

It is known that the superconducting electronic specific heat C_e is sensitive to the low-energy excitation of quasiparticles in superconductors, providing a reliable examination for the possible mixture of spin singlet and triplet states in noncentrosymmetric superconductors. Here, the temperature variation of $C_e(T)$ can be obtained by $C_e(T) = C(T) - \beta T^3 - \delta T^5$ and the result of C_e/T versus T/T_c at $H = 0$ is illustrated in figure 9. The electronic specific heat jump ΔC_e can be employed to measure the strength of the electron-phonon coupling via the ratio of $\Delta C_e/\gamma T_c$. Taking $\Delta C_e/T_c = 169 \text{ mJ mol}^{-1} \text{ K}^{-2}$ and $\gamma = 111.8 \text{ mJ mol}^{-1} \text{ K}^{-2}$, we obtained the value of $\Delta C_e/\gamma T_c = 1.51$, which is slightly higher than the BCS value of 1.43 predicted for a weakly coupled superconductor. With this respect, this result implies a moderate electron-phonon coupling in $\text{Re}_{24}\text{Ti}_5$ without any model fitting.

As indicated from figure 9, the T -dependent feature of C_e/T behaves similarly to those of the typical s-wave

Table 1. Parameters for normal and superconducting states of $\text{Re}_{24}\text{Ti}_5$.

Parameter	Unit	$\text{Re}_{24}\text{Ti}_5$	$\text{Re}_{23.8}\text{Nb}_{5.2}$ [9]
T_c	K	5.8	8.8
ρ_o	$\mu\Omega \text{ cm}$	214.7	189
A	$\mu\Omega \text{ cm K}^{-2}$	0.022	0.007
T_F	K	22 400	
$N(E_F)$	states eV^{-1} f.u. $^{-1}$	14.85	6.56
$\mu_0 H_{c2}(0)$	T	10.75	17.3
γ	$\text{mJ mol}^{-1} \text{ K}^{-2}$	111.8	53.4
β	$\text{mJ mol}^{-1} \text{ K}^{-4}$	1.47	2.05
θ_D	K	428	383
λ_{ep}		0.6	0.73
$\Delta C_e/T_c$	$\text{mJ mol}^{-1} \text{ K}^{-2}$	169	100
$\Delta C_e/\gamma T_c$		1.51	1.86
Δ/k_B	K	10.6	16.1
$2\Delta/k_B T_c$		3.68	3.67

superconductors. We thus employed the BCS formula for $C_e(T)$ to fit the result of C_e/T with the fitting curve also displayed in figure 9. The fitting result is quite satisfactory, yielding an isotropic gap Δ/k_B of about 10.6 K for $\text{Re}_{24}\text{Ti}_5$. Also the superconducting transition temperature of 5.74 K revealed from the fit is close to those from the transport and magnetic measurements. The entropy conservation required for a second-order phase transition is fulfilled, as shown in the inset of figure 9. This check warrants the thermodynamic consistency for both the measured data and the determination of $C(T)$. From the values of Δ and T_c , it yields a dimensionless ratio of $2\Delta/k_B T_c = 3.68$, which is almost identical to the value of 3.67 obtained from the analysis of the electronic specific heat data in $\text{Re}_{0.82}\text{Nb}_{0.18}$ [9]. In addition, this result is comparable to those in other fully gapped noncentrosymmetric superconductors, such as 3.52 for Re_3W and 3.6 for Ru_7B_3 [7, 24].

According to our $C_e(T)$ analysis, $\text{Re}_{24}\text{Ti}_5$ is better described as an ordinary s-wave superconductor, indicating that a mixture of the spin singlet and triplet states in the SC phase driven by the ASOC effect is invisible. This result is likely due to a small band splitting lifted by ASOC as compared to the transition temperature $T_c \simeq 5.8$ K for $\text{Re}_{24}\text{Ti}_5$. On the other hand, Mineev and Samokhin have argued that the effects of nonmagnetic impurities on noncentrosymmetric superconductors may lead to an inevitable consequence of the band splitting even though the intrinsic ASOC is stronger than SC energy scales [31]. Such an extrinsic effect could mask the underlying SC gap anisotropy in the present case of $\text{Re}_{24}\text{Ti}_5$.

3. Conclusions

The physical characteristics of the noncentrosymmetric superconductor $\text{Re}_{24}\text{Ti}_5$ have been established from this study. In the normal state, the electronic features exhibit ordinary metallic behavior. In the superconducting state, $\text{Re}_{24}\text{Ti}_5$ behaves as a typical s-wave superconductor, implying that the anticipated ASOC effect in this material is quite weak and/or suppressed by other effects. Furthermore, with the comparison of the present observations to those of

$\text{Re}_{23.8}\text{Nb}_{5.2}$, a strong similarity was found for these two systems. On this basis, we point to the uniformity in both normal and superconducting properties for the Re-based superconductors with the noncentrosymmetric α -Mn crystal structure.

Acknowledgments

Acknowledgment is made to the National Science Council of Taiwan for supporting of this research under Grant Nos. NSC-101-2112-M-006-009-MY2 (CSL), NSC-101-2112-M-009-017-MY2 (JYL), and NSC-100-2112-M-259-002-MY3 (YKK).

References

- [1] Edelstein V M 1995 *Phys. Rev. Lett.* **75** 2004
- [2] Gorkov L P and Rashba E I 2001 *Phys. Rev. Lett.* **87** 037004
- [3] Frigeri P A, Agterberg D F, Koga A and Sigrist M 2004 *Phys. Rev. Lett.* **92** 097001
- [4] Samokhin K V 2005 *Phys. Rev. Lett.* **94** 027004
- [5] Bauer E, Hilscher G, Michor H, Paul Ch, Scheidt E W, Grabinov A, Seropgin Yu, Noel H, Sigrist M and Rogl P 2004 *Phys. Rev. Lett.* **92** 027003
- [6] Mukuda H, Ohara T, Yashima M, Kitaoka Y, Settai R, Onuki Y, Itoh K M and Haller E E 2010 *Phys. Rev. Lett.* **104** 017002
- [7] Zuev Y L, Kuznetsova V A, Prozorov R, Vannette M D, Lobanov M V, Christen D K and Thompson J R 2007 *Phys. Rev. B* **76** 132508
- [8] Biswas P K, Lees M R, Hillier A D, Smith R I, Marshall W G and Paul D McK 2011 *Phys. Rev. B* **84** 184529
- [9] Karki A B, Xiong Y M, Haldolaarachchige N, Stadler S, Vekhter I, Adams P W, Young D P, Phelan W A and Chan J Y 2011 *Phys. Rev. B* **83** 144525
- [10] Lue C S, Su T H, Liu H F and Young B-L 2011 *Phys. Rev. B* **84** 052509
- [11] Bauer E et al 2010 *Phys. Rev. B* **82** 064511
- [12] Karki A B, Xiong Y M, Vekhter I, Browne D, Adams P W, Young D P, Thomas K R, Chan J Y, Kim H and Prozorov R 2010 *Phys. Rev. B* **82** 064512
- [13] Kuo C N, Liu H F and Lue C S 2012 *Phys. Rev. B* **85** 052501
- [14] Mondal M, Joshi B, Kumar S, Kamlapure A, Ganguli S C, Thamizhavel A, Mandal S S, Ramakrishnan S and Raychaudhuri P 2012 *Phys. Rev. B* **86** 094520
- [15] Trzebiatowski W and Niemiec J 1955 *Roczniki Chem.* **29** 277
- [16] Matthias B T, Compton V B and Corenzwit E 1961 *J. Phys. Chem. Solids* **19** 130
- [17] Matthias B T, Geballe T H and Compton V B 1963 *Rev. Mod. Phys.* **35** 1
- [18] Steadman R and Nuttall P M 1964 *Acta Crystallogr.* **17** 62
- [19] Savitskii E M, Baron V V, Efimov Yu V, Bychkova M I and Myzenkova L F 1966 *Superconducting Materials* (New York: Plenum)
- [20] Lue C S, Yang S H, Abhyankar A, Hsu Y D, Hong H T and Kuo Y K 2010 *Phys. Rev. B* **82** 045111
- [21] Barnard R D 1972 *Thermoelectricity in Metals and Alloys* (London: Taylor and Francis)
- [22] Werthamer N R, Helfand E and Hohenberg P C 1966 *Phys. Rev.* **147** 295
- [23] Lan M D, Chang J C, Lu K T, Lee C Y, Shih H Y and Jeng G Y 2001 *IEEE Trans. Appl. Supercond.* **11** 3607
- [24] Fang L, Yang H, Zhu X, Mu G, Wang Z-S, Shan L, Ren C and Wen H-H 2009 *Phys. Rev. B* **79** 144509
- [25] Kittel C 2005 *Introduction to Solid State Physics* 8th edn (New York: Wiley)
- [26] McMillan W L 1968 *Phys. Rev.* **167** 331
- [27] Poole C P Jr (ed) 1999 *Handbook of Superconductivity* (New York: Academic) p 478 (Chapter 9, Sec. G)
- [28] Klimczuk T et al 2012 *Phys. Rev. B* **85** 174505
- [29] Klimczuk T, Ronning F, Sidorov V, Cava R J and Thompson J D 2007 *Phys. Rev. Lett.* **99** 257004
- [30] Anand V K, Hillier A D, Adroja D T, Strydom A M, Michor H, McEwen K A and Rainford B D 2011 *Phys. Rev. B* **83** 064522
- [31] Mineev V P and Samokhin K V 2007 *Phys. Rev. B* **75** 184529